NUMERICAL ERRORS IN GROUNDWATER AND OVERLAND FLOW MODELS

A. M. Wasantha Lal

Lead Engineer

South Florida Water Management District

3301 Gun Club Road

West Palm Beach, FL 33406

ABSTRACT

Numerical error estimates are useful to evaluate the applicability of overland and groundwater flow models, and verify the validity of their results. In this paper, methods of estimating numerical errors are developed, and then applied to evaluate the numerical accuracy of the South Florida Water Management Model SFWMM. Analytical expressions for errors generated during the propagation of disturbances due to well pumping, boundary water-level changes and rainfall are obtained for steady and transient conditions using Fourier analysis of the linearized governing equations. Different situations under which truncation errors are introduced into models, and their variation with the spatial and temporal discretization are discussed. Numerical experiments are carried out with the MODFLOW model, and a number of implicit and explicit models to verify the results. Dimensionless parameters are used in the expressions so that the results can be used to determine discretization errors in in any existing or new finite difference model of regional or local scale.

INTRODUCTION

The number of computer models used to simulate various overland flow and groundwater flow conditions has increased recently due to the increased need to analyze environmental, agricultural and developmental issues. In South Florida, models of different scales are used for planning, management and regulation of water resources. Regional models are used mostly to address issues related to planning and management of water resources, while medium and small scale models, with county-wide and local coverages, are used for regulatory and permitting applications. The multi-agency efforts to implement the restoration of the Everglades have also increased the interest in, and requirement for various modeling efforts. As a result of the multiple and overlapping use of models, the need to understand, and properly apply and interpret the results of these models has increased greatly. The current study is aimed at understanding the relationships among spatial and temporal discretizations, and numerical errors of groundwater and surface water models. Both steady and unsteady cases are investigated for a variety of applications used in South Florida.

Most groundwater and overland flow models are based on applying a numerical method to solve a parabolic partial differential equation that is sometimes referred to as the diffusion equation. Diffusion flow models of varying resolutions are used to examine hydrologic processes at different scales. Numerical models of any scale contain uncertainties due to inaccuracies in the inputs, parameters, and algorithms. Input uncertainty is due to inaccurate or inadequate spatial and temporal input data such as rainfall, and evapotranspiration. This cause of uncertainty can be reduced by improving the data quality and the density of the data collection network. Parameter

uncertainty is mainly due to inaccurate values of spatially varying physical characteristics. This error can be reduced somewhat by calibration (Neuman, 1973, Willis and Yeh, 1987, Lal, 1995). Numerical errors are considered to be the source of algorithm uncertainty discussed in the present paper. Various unconditionally stable numerical methods using implicit or other methods have made it possible for modelers to use almost any discretization with computer models. Unlike explicit methods, where there is some error control because of the stability condition, implicit models such as MODFLOW need guidelines to select discretizations so that the error is known and controlled.

Richtmyer and Morton (1967) have compiled many of the basic developments behind consistency, convergence and stability of parabolic and other problems. In many of the early applications, the primary method of numerical error control is to use a discretization that satisfies the stability conditions derived using Von Neuman and other methods. Error analysis of partial differential equations generally provides an order-of-magnitude estimate. Error control is commonly used when solving initial value problems that involve ordinary differential equations, as in the Runge-Kutta-Fehlberg method and the Adams variable step-size predictor-corrector method (Burden and Fairs, 1985). Anderson and Woessner (1991) suggested that empirical methods based on model convergence should be applied to control numerical errors in MODFLOW applications. Hirsch (1989) used a method for error analysis based on linearization and Fourier Analysis. This method, which is similar to the Von Neuman method for stability analysis, has been used for diffusion and other equations. Lal (1998) used the same method with additional expressions derived for compu-

tational time to evaluate and compare the computational performances of various numerical models used to solve diffusion equations. The subject of error analysis and output evaluation has become increasingly important because the space and time discretizations used in some model applications are arbitrarily chosen. The use of unconditionally stable implicit methods has also complicated the use of the stability condition as an error control. The current study extends the ideas of Fourier analysis used by Hirsch (1989) and Lal (1998a) to develop expressions for numerical errors of many groundwater flow and overland flow models.

Numerical errors are introduced when the solution to the governing partial differential equations is represented by discrete values in the model, and when these discrete values are used in numerical computations in the finite difference method. Numerical errors introduced in the representation of data and during computations are discussed in the present paper. Stresses and errors due to conditions common in South Florida such as variable water levels in canals, variable pumping rates in wells, and variable rainfall are analyzed separately. The principle of superposition makes it possible to combine these cases. The error analysis is conducted for an arbitrary Fourier component and the steady state. The results are presented in dimensionless forms and verified using MODFLOW and other models. The results can be used in a wide variety of practical problems to determine numerical error. An application of the method is presented to demonstrate the evaluation of an overland flow model and a groundwater flow model for South Florida.

NUMERICAL SOLUTION OF THE DIFFUSION EQUATION

Two dimensional groundwater flow and overland flow can be explained using the following gov-

erning equation. For overland flow, the equation is derived by neglecting the inertia terms in the St Venant equations. (Hromadka and Lai, 1985, Lal, 1998).

$$s_c \frac{\partial H}{\partial t} = \frac{\partial}{\partial x}\left(K\frac{\partial H}{\partial x}\right) + \frac{\partial}{\partial y}\left(K\frac{\partial H}{\partial y}\right) + S \tag{1}$$

in which, $H = h + z =$ water level or water head; $S =$ source and sink terms representing rainfall, evapotranspiration and infiltration. For overland flow, $h =$ water depth; $K = \frac{h^{\frac{5}{3}}}{n_b\sqrt{S_n}}$ when the Manning's equation is used; $n_b =$ Manning's coefficient; $S_n =$ water surface slope and $s_c = 1$. For groundwater flow, $s_c =$ storage coefficient; $K =$ transmissivity of the aquifer, assuming an isotropic material; $K \approx k_c\bar{h}$ for unconfined flow in which $\bar{h} =$ water depth of the saturated layer and $k_c =$ hydraulic conductivity. The flow vector is computed using

$$\vec{Q} = K\vec{\nabla}H \tag{2}$$

in which, $\vec{Q} =$ flow vector giving flow rate per unit width. When a weighted implicit finite volume formulation is used, (1) can be expressed for an arbitrary cell as (Lal, 1998)

$$H_{i,j}^{n+1} = H_{i,j}^{n} + \alpha\, Q_{net}(H^{n+1})\frac{\Delta t}{s_c \Delta A} + (1-\alpha)\, Q_{net}(H^{n})\frac{\Delta t}{s_c \Delta A} + \frac{\bar{S}\Delta t}{\Delta A} \tag{3}$$

in which $\Delta A =$ area of the cell; $Q_{net} =$ net inflow to the cell; $\alpha =$ weighting factor for semi-implicit schemes; $n =$ time step; $\bar{S} =$ weighted average source term for the area during the time step. For the rectangular grid used in the study, $Q_{net}(H)$ is given by

$$Q_{net}(H) = K_{i+\frac{1}{2},j}(H_{i+1,j} - H_{i,j}) + K_{i-\frac{1}{2},j}(H_{i-1,j} - H_{i,j})$$
$$+K_{i,j+\frac{1}{2}}(H_{i,j+1} - H_{i,j}) + K_{i,j-\frac{1}{2}}(H_{i,j-1} - H_{i,j}) \quad (4)$$

Explicit and the implicit methods are obtained by using $\alpha = 0$ and 1.0 with (3) and (4).

NUMERICAL ERROR ANALYSIS

Numerical errors are present in computer models because of the use of discrete values to represent continuous functions explaining flow conditions, and the use of numerical methods to approximately solve the governing equations. Texts by Richtmyer and Morton (1967) and Sod (1985) are two of the early and recent books that describe the general methods of Fourier analysis and complex analysis used in analyzing numerical methods, and in analyzing errors in the current paper. Hirsch (1989) described the adaptation of some of these methods of stability analysis to error analysis.

In this paper, errors are considered to be introduced in three different ways even if they can all be classified as truncation errors.

(A) Errors are introduced when the initial and boundary condition data are recorded and provided to the model as discrete values in time and space. Due to this type of error in ”representation”, spectral components in the solution with frequencies or wave numbers above a certain value are either completely truncated, or not represented accurately.

(B) Errors are introduced if the internal discretization of the model is not sufficient to carry the

solution over the entire time and space domain. For example, even if the time step is sufficient to describe a boundary disturbance, if the spatial discretization is inadequate at any point in its path, the solution may not propagate accurately.

(C) Numerical errors are also introduced when computations are carried out using the Fourier components that are left over and did not vanish due to reasons given in (A) and (B). Computer models are based on numerical approximations for derivatives, etc. They use finite differences and other methods for these approximations. The truncation errors resulting from these approximations are considered here, and are computed using Fourier analysis.

Higher frequency components in the solution are subjected to these errors more than the lower frequency components. They will be quantified using an arbitrary Fourier component of the solution. Assuming that a component can be described using its wave number k ($k = 2\pi/$ wavelength) or frequency f ($f = 2\pi/$ period), the following approximate expressions were obtained for time or space discretization errors (A) and (B) of 1-D and 2-D problems. A Monte Carlo method was used to determine these errors by representing a large number of different 1-D and 2-D wave shapes with random wave numbers and random phase shifts using a uniform grid, and estimating the maximum errors between the true solution and the linearly interpolated grid–based solution.

$$\phi = 0.5\sqrt{\varepsilon_d} \quad \text{or} \quad \varepsilon_d = 4.0\,\phi^2 \quad \text{for 1-D} \tag{5}$$

$$\phi = 0.35\sqrt{\varepsilon_d} \quad \text{or} \quad \varepsilon_d = 7.8\,\phi^2 \quad \text{for 2-D} \tag{6}$$

in which, $\varepsilon_d =$ maximum percentage discretization error. The spatial discretization error ε_d exists even with the smallest time steps possible. $\phi = k\Delta x$ is the dimensionless form of Δx. The same

equation applies for time discretizations when ϕ is replaced with ψ in which $\psi = f\Delta t$. Quantity ϕ was also used by Hirsch (1989) to make Δx dimensionless. ε_d only depends on the geometrical shape of the wave form. For 1-D problems, 1% and 5% errors in discretization, for example, correspond to ϕ or ψ equal to 0.5 and 1.1 respectively. For 2-D problems, they correspond to ϕ or ψ equal to 0.35 and 0.80 respectively. An easier way to visualize ϕ or ψ is to consider that approximately $\frac{\pi}{\phi}$ grid spaces or discretizations are needed to describe half the wave length of a sine wave. It can be seen that approximately six grid spaces are needed over the length of half a sine wave to represent it so that the maximum error is $< 1\%$. Three discretizations per half sine wave or $\phi = 1.05$ makes the maximum error $< 4.5\%$. Equation (6) can also be obtained using actual model runs (Lal, 1998a).

The error explained in (B) can be understood by realizing that k and f of a single Fourier component are related as a result of the governing equations. The relationship between f and k can be obtained for diffusion flow using solutions of the form $H = H_0 e^{I(kx-ft)}$ and $H = H_0 e^{I(kx+ky-ft)}$ respectively for 1-D and 2-D problems in which $I = \sqrt{-1}$. In the case of 2-D problems, k is assumed to be the same in both x and y directions for simplicity. Substituting the above forms of the solution in the governing equations, it can be shown that wave number k of a sinusoidal water level variation in a semi-infinite aquifer is related to the disturbing frequency f by

$$f = d\frac{K}{s_c}k^2 \tag{7}$$

in which, $d = 1$ and 2 for 1-D and 2-D problems respectively. For a problem with a constant disturbance $H = H_0 \sin(ft)$ maintained at the boundary, the same solution is true with $d = 2$ and 4 for

1-D and 2-D problems.

Computational errors

To estimate computational errors (C), the behavior of the numerical scheme in response to an arbitrary i th harmonic with a wave number $k_i = \frac{i\pi}{N}$ is compared with the behavior of the governing equation with respect to the same harmonic. In the equation, $N = L/\Delta x$ in which L is the length of the domain in x direction. A grid spacing of Δx would allow a minimum wave length $\lambda_{min} \approx 2\Delta x$ and a maximum wave length $\lambda_{max} \approx 2L$. In the analysis, a term ϕ_i defined as $\phi_i = k_i \Delta x$ is used to represent the i th harmonic in dimensionless form (Hirsch, 1989). The subscript is often removed for simplicity. A term $\psi = f\Delta t$ can be defined similarly to represent a harmonic in the time domain, in which the frequency $f = 2\pi/T_p$, and $T_p =$ wave period. ϕ is used as the dimensionless variable to describe the spatial discretization.

For numerical methods based on finite differences, an analytical expression can be derived for the numerical error (Hirsch, 1989, Lal, 1998).

$$\varepsilon = 1 - |G| \tag{8}$$

in which, $\varepsilon =$ magnitude of the analytically computed numerical error per time step as a fraction of the amplitude; $G =$ ratio of amplitudes of numerical and analytical solutions, or the amplification factor of the numerical method.

$$G = \frac{1 - 4d(1-\alpha)\beta \sin^2(\phi/2)}{1 + 4d\alpha\beta \sin^2(\phi/2)} \frac{1}{e^{-d\beta\phi^2}} \tag{9}$$

$\beta = \frac{K\Delta t}{s_c \Delta x^2}$ = non-dimensional form of Δt; $d = 1, 2$ for one and two dimensional problems with

square grids. Equation (8) which is derived assuming the analytical solution (7) (Hirsch, 1989) can be expanded to give

$$\varepsilon = \pm\frac{d^2\beta^2\phi^4}{2} + \frac{d\beta\phi^4}{12} + \ldots = \pm\frac{d^2k^4K^2\Delta t^2}{2\,s_c^2} + \frac{dKk^4\Delta t\Delta x^2}{12\,s_c} + \ldots \tag{10}$$

in which $+$ and $-$ signs correspond to implicit and explicit models respectively. The cumulative numerical error after many time steps, ε_T, depends on the number of time steps n_t, and the error at each time step ε. Error ε_T is bounded by $n_t\varepsilon$, in which $n_t = T/\Delta t$. This bound is obtained by assuming that the errors are additive. In the sine cycle, these errors are additive for half the cycle and subtractive for the other half. The bound is

$$\varepsilon_T \approx \frac{\varepsilon}{\beta\phi^2}\frac{TKk^2}{s_c} = \frac{\varepsilon}{d\beta\phi^2}fT \tag{11}$$

where, $k =$ wave number of the harmonic; $T =$ maximum duration over which a given harmonic stays in the computational domain and accumulates errors. Examples shown below demonstrate how fT is computed. In the problem of a water level variation driven by a stationary rainfall pattern, $fT = \pi/4$ because the error is largest after a quarter cycle. In the problem of a water level disturbance at the boundary of a semi-infinite aquifer, the disturbance travels at a speed of f/k, and covers a distance X in time T making $fT = kX$. It can be shown using (16) described later that the absolute error in this problem is maximum when $fT = 1$. Similarly it can be shown that $fT < 3$ for most practical applications for which error $< 5\%$.

Equation (11) can be simplified by using a truncated Taylor series expansion. For explicit,

implicit and semi-explicit 1-D and 2-D finite difference models,

$$\varepsilon_T \quad \text{(expl/impl 1-D)} \quad \approx \quad \frac{fT\phi^2}{2}(\mp\beta - \frac{1}{6}) \tag{12}$$

$$\varepsilon_T \quad \text{(semi-impl 1-D)} \quad \approx \quad fT\left[\frac{\phi^2}{12} - \frac{\phi^4}{12}(\beta^2 - \frac{1}{30})\right] \tag{13}$$

$$\varepsilon_T \quad \text{(expl/impl 2-D)} \quad \approx \quad fT\phi^2(\pm\beta - \frac{1}{12}) \tag{14}$$

$$\varepsilon_T \quad \text{(semi-impl 2-D)} \quad \approx \quad fT\left[-\frac{\phi^2}{6} + \frac{2\phi^4}{3}(\beta^2 + \frac{1}{120})\right] \tag{15}$$

The positive and negative signs apply for the explicit and implicit methods respectively. Semi-implicit methods use $\alpha = 0.5$. Explicit 1-D and 2-D models additionally require $\beta < 0.5$ and $\beta < 0.25$ respectively for stability. Numerical experiments will later show that offsets of β such as $1/6$ and $1/12$ in (12) and (13) can be neglected especially with implicit methods using relatively large β. The above equations also show that semi-implicit methods are second order accurate in time because β is to the second power.

PROPAGATION OF ERRORS

When the water level in a canal, tidal bay or the ocean varies, a disturbance in head is created which travels away from the source of the disturbance. Water level changes due to such stresses constitute an important part of the solution in many models. To understand numerical errors in such solutions, propagation of a sinusoidal disturbance $H = H_0 \sin(ft)$ in a semi-infinite aquifer is studied in 1-D. It can be shown that the analytical solution for head in such a semi-infinite medium is

$$H(x,t) = H_0 e^{-kx} \sin(ft - kx) \tag{16}$$

in which, $f = 2Kk^2/s_c$ according to (7). The analytical solution for discharge is given by

$$Q(x,t) = \sqrt{2}KkH_0 e^{-kx} \sin\left(kx - ft - \frac{\pi}{4}\right) \tag{17}$$

Equation (16) shows that the amplitude H becomes less than 1%, 5% and 37% of the starting amplitude H_0 when $fT = kX > 5$, 3 and 1 respectively in which T and X are described earlier as the time or the distance of evolution over which errors accumulate. These values show that the waveforms become negligible after traveling about one cycle. Instead of the fixed percentages such as 1% or 5%, if the decayed amplitude is expressed as a fraction α_d of the original amplitude in (16), the ratio of the amplitudes of $H(x,t)$ and H_0 or $\exp(-kx) = \alpha_d$ can be used to express the exact solution (7) as

$$\frac{s_c X^2}{KT_p} = \frac{(\ln \alpha_d)^2}{\pi} \quad \text{or} \tag{18}$$

$$\frac{KT}{s_c L_p^2} = -\frac{\ln \alpha_d}{8\pi^2} \tag{19}$$

in which, $T_p =$ period of the wave; $L_p =$ wave length. These equations are similar to the equations derived by Townley (1995) and used by Haitjema (1995) for transient state analysis. They can be used to determine the length and the time scales of a disturbance in a porous medium when the disturbance has a period T_p or a wave length L_p. The numerical error at a distance x from the point of disturbance is computed using (11) and $fT = kX$ as discussed earlier.

$$\varepsilon_T(x) = \frac{k\varepsilon}{\beta\phi^2} x \tag{20}$$

This equation shows that as a percentage, the numerical error increases linearly with x. Since water level fluctuations decrease exponentially, the absolute error first increases and then decreases with

the distance, giving a maximum ε_T of approximately $0.37\phi^2\beta$, at $fT = kX = 1$.

In order to verify the accuracy of the analytical estimates for numerical error, ε values were computed for a 1-D semi-infinite problem using both analytical and numerical methods. The numerical experiment involved studying the decay of the amplitude of a sinusoidal boundary disturbance with distance. The error in the amplitude of the numerical model ε_T was determined by subtracting the analytical amplitude from the amplitude obtained for the numerical model. Equations (16) and (17) were used to compute analytical amplitudes. The graph of ε_T against x is obtained by subtracting the analytical amplitude envelope from the model amplitude envelope. To obtain the model amplitude envelope, over 1000 cycles of sine waves were passed through the domain first until a sufficiently steady initial initial condition is reached. Then, the envelope was determined by sending over 200 sine waves until a fairly steady envelope curve is formed. Figure 1 shows one such amplitude envelope for the MODFLOW model ($\phi = 0.8$, $\beta = 0.78$) and its graph of ε_T versus number of grids points from the boundary, when the total number of equally spaced grid points is 100. Errors at the sine wave peaks (maximums) and troughs (minimums) are both shown. The graph of ε_T versus x is approximately straight near the boundary, and has a gradient $k\varepsilon/(\beta\phi^2)$ according to (20). Model values of ε can be obtained for various computer models using this gradient. Each of the numerical experiments leads to one point in the ε versus β plot. Since dimensionless parameters are used, the actual physical dimensions and physical constants used in the tests are not important. The analytical plot of ε versus β was obtained using (8). Explicit, semi-implicit and the fully implicit MODFLOW models values were obtained using $\alpha = 0.0$, 0.5

and 1.0 with $d = 1$.

Figures 2, 3 and 4 show the ε values observed in the ADI, explicit and the MODFLOW(PCG2) models respectively and the corresponding analytical values. A range of ϕ values such as 0.2, 0.4 and 0.8 were used in the experiments. All the figures show that the analytical and numerical plots of ε agree very closely, implying that the analytical expressions derived for numerical error are accurate for the models investigated. These results are similar to the results shown by Lal (1998a) obtained using a water level subsidence experiment. Figure 3 shows that the error measured as the (numerical value – analytical value) is small when $\beta \approx 0.16$, and becomes negative when $\beta < 0.16$. The dashed line in Figure 3 shows that the approximate form of the analytical solution in (12) based on a truncated Taylor series is also relatively accurate. The behavior of error with β and ϕ for a problem with a triangular mesh is demonstrated in the paper by Lal (1998b).

NUMERICAL ERRORS OF FLOW VELOCITY AND DISCHARGE

In overland flow and groundwater flow models based on the diffusion equations, discharge across two neighboring cells is

$$Q^n_{i+1/2,j} = K\frac{H^n_{i+1,j} - H^n_{i,j}}{\Delta x} \tag{21}$$

in which, $H^n_{i,j}$ and $H^n_{i+1,j}$ are the heads of the cells; $Q^n_{i+\frac{1}{2},j}$ = flow rate betweens cells per unit width. In order to compute the numerical error in the flow, a solution for a Fourier component of the form $H^n_i = H^n_0 \exp(I\phi i)$ is substituted in (21) to obtain $Q^n_{i+1/2} = 2KH^n_0 I \sin(\phi/2)/\Delta x$. Using an analytical solution of the form $H(x,t) = H_0 \exp(-Kk^2 t)\exp(Ikx)$ for which the numerical solution is H^n_i, the governing equation can be used to obtain the analytical flow rate as $Q(x,t) = KkIH(x,t)$. The ratio between numerical and analytical amplitudes of $Q^n_{i+1/2}$ and $Q(x,t)$ can now be used to compute the numerical error as $\varepsilon_Q = 1 - 2|G|\sin(\phi/2)/\phi$ in which $|G|$ in (8) is computed as $H^n_i/H(x,t)$. ε_Q can be related to ε for small ϕ using the approximate relationship

$$\varepsilon_Q \approx \varepsilon\frac{2\sin(\frac{\phi}{2})}{\phi} \tag{22}$$

in which ε_Q = numerical error in discharge for one time step, as a fraction of the analytical discharge for the specific Fourier component. Numerical errors in flow velocity and discharge are given by the same expression. Comparison of (8) with (22) shows that the error in the head and the discharge are approximately the same, with the former slightly higher.

The accuracy of (22) can be verified in the same way it was done for the head, by simulating the propagation of sinusoidal disturbances in head, and observing the decay of the amplitudes of the sinusoidal discharge rate with distance. This method is similar to the method used for errors in

head. The method is started by first running a model for a long period of time, passing over 10000 cycles of waves until a fairly steady wave shape is established as the initial condition. Errors are computed by assuming the analytical solution (17) to be exact. The gradient of the error versus distance curve is used as before to compute ε_Q for the model. Figure 5 shows a plot of ε_Q with β for a fully implicit model ($\alpha = 1$) when $\phi = 0.5$, 1.0, and 1.5. According to the figure, the analytical estimates of error compare well with the values observed in the models.

NUMERICAL ERRORS NEAR WELLS UNDER VARIABLE PUMPING RATES

Numerical errors of model results are large close to groundwater wells because of the extreme curvature in the solution. The Thiem equation provides an approximate but efficient method to compute water levels very close to a well when the water level of the cell is known (Anderson and Woessner, 1991). Numerical error at and near a cell containing a well subjected to a variable pumping rate is investigated in this section. The results are useful in selecting the optimal discretization for new models, and in evaluating the output of existing models. All the formulas are derived for an arbitrary Fourier component of the pumping rate time series. The well is assumed to be circular, and situated at the center of a square cell to simplify the derivations. Even if some of these assumptions may not be true in the actual application, results of the study are useful in understanding the behavior of numerical errors near wells.

The following equation governing groundwater flow around a well is used for the analysis.

$$s_c \frac{\partial H}{\partial t} = \frac{K}{r} \frac{\partial}{\partial r} (r \frac{\partial H}{\partial r}) \tag{23}$$

Consider a solution in the form $H = R(r)T(t)$ in which $T(t) = \exp(Ift)$. Using separation of

variables, (23) can be reduced to

$$r^2\frac{d^2R}{dr^2}+r\frac{dR}{dr}-\frac{IfRr^2s_c}{K}=0 \tag{24}$$

Using a characteristic length $\lambda=\sqrt{K/(fs_c)}$, radius r can be made dimensionless as $\hat{r}=r/\lambda$. Similarly, t can be made dimensionless using $\hat{t}=ft$. The general solution of (24) that is also finite at $\hat{r}\to\infty$ can be expressed as

$$H(\hat{r},\hat{t})=cK_o(\hat{r})\exp(I\hat{t}) \tag{25}$$

in which $K_o(\hat{r})$ is a modified Bessel function; $c=$ a constant that has to be determined for the specific problem with specific boundary conditions. Consider a well of radius r_w pumped with a sinusoidal pumping rate $Q(t)=Q_0\sin(\hat{t})$. The constant c can be determined by assuming that $Q(t)=$ flow rate at $\hat{r}=\hat{r}_w$ of the solution in (25) in which $\hat{r}_w=$ dimensionless well radius. This assumption is valid for most wells in South Florida where the storage capacity of the well is negligible. Substituting c into (25), it is possible to obtain the analytical solution of the pumping problem as

$$H(\hat{r},\hat{t})=\frac{s_cQ_0K_o(\hat{r})}{2\pi K\hat{r}_wK_1(\hat{r}_w)}\sin(\hat{t}) \quad \text{for} \quad \hat{r}>\hat{r}_w \tag{26}$$

In the case of extremely small diameter wells, $\hat{r}_wK_1(\hat{r}_w)\to 1$ as $\hat{r}_w\to 0$, and (26) becomes

$$H(\hat{r},\hat{t})=\frac{s_cQ_0K_o(\hat{r})}{2\pi K}\sin(\hat{t}) \tag{27}$$

Equation 26 shows that the amplitude decays rapidly with distance as exhibited by the behavior of K_o. Equation 26 is used as the exact solution when computing the numerical error in a square finite difference cell. Table 1 shows the variation of the portion $K_0(\hat{r})/(\hat{r}_wK_1(\hat{r}_w))$ of (26) as an indicator of this amplitude. The table shows the influence of the well; for example, when $\hat{r}>2.75$

and $\hat{r}_w$ =0.5 or less, the amplitude of the water level fluctuation will decay to less than 5%. When $\hat{r}_w$ =0.1, then $\hat{r} > 1.95$ for the amplitude to decay to 5%.

In order to determine the numerical error in a model when used to simulate pumping, a $\Delta x \times \Delta x$ square cell containing the well is simulated by approximating it as an axisymmetric problem. The square cell is approximated as a circular area of an equivalent radius. The head at this radius is considered as the model head for that cell. The equivalent problem is solved by assuming the solution to be in the form (25) with a value of c to be determined using a water balance equation. Integral form of the continuity equation for the cell is as shown below, in which the first term is the pumping rate, the second term is the seepage rate through the cell wall, and the third term is the rate of change of total water volume in the cell.

$$-Q(t) + 2\pi r_c K \left(\frac{\partial H}{\partial r}\right)_{r=r_c} \approx \int_{r=0}^{r_a} 2\pi r s_c \frac{\partial H}{\partial t}\, dr \tag{28}$$

in which a radius $r_c = a_c \Delta x$ is used to compute the approximate seepage rate into the $\Delta x \times \Delta x$ cell. Anderson and Woessner (1991) used r_c as the radius of a well at which the drawdown for pumping rate $Q(t)$ is given by the numerical solution based on a grid spacing Δx. The radius $r_a = a_a \Delta x =$ radius at which the square cell area is equal to the area of the circle. The value of a_c is 0.208 (Anderson and Woessner, 1991), and the value of a_a is 0.564 because $\Delta x^2 = \pi r_a^2$. The pumping rate is assumed as $Q(t) = Q_0 \sin(ft)$. The value of c obtained by substituting (25) into (28) is used in (25) to obtain the head in the numerical model as

$$H_c(\hat{r},\hat{t}) = \frac{s_c Q_0 K_o(\hat{r}) \sin(\hat{t} - \hat{t}_o)}{2\pi K \hat{r}_c K_1(\hat{r}_c) \sqrt{\left[1 + \left(\frac{M_o(\hat{r}_a)}{\hat{r}_c K_1(\hat{r}_c)}\right)^2\right]}} \quad \text{for} \quad \hat{r} \geq \hat{r}_c \tag{29}$$

in which, $M_o(r_a)$ is defined as

$$M_o(\hat{r}_a) = \int_0^{\hat{r}_a} \hat{r} K_o(\hat{r})\, d\hat{r} \tag{30}$$

$\hat{t}_0 =$ a time lag error which is not investigated further in the current study. Value of $H = H_c$ obtained at $\hat{r} = \hat{r}_c$ in (29) is considered as the numerical value of the cell containing the well. The exact solution is given by (26) at a radius $\hat{r} = \hat{r}_c = 0.208\Delta x$. They differ in amplitude and phase. The difference in amplitude is used to compute the approximate numerical error by first computing the ratio C_c between the amplitudes of the numerical and exact solutions. The approximate error in amplitude is $\varepsilon_w = 100(1 - C_c)$, compared to a well of effective radius r_c. Using (29) and (26), C_c can be expressed as

$$C_c = \frac{1}{\sqrt{\left[1 + \left(\frac{M_o(\hat{r}_a)}{\hat{r}_c K_1(\hat{r}_c)}\right)^2\right]}} \tag{31}$$

To compute the numerical values of ε_w, $\hat{r}_c = a_c \Delta x \sqrt{(fs_c/K)}$ and $\hat{r}_a = a_a \Delta x \sqrt{(fs_c/K)}$ are used with $a_c = 0.208$ and $a_a = 0.564$. Table 2 shows the values of ε_w obtained for various values of $\Delta x \sqrt{(fs_c/K)}$. It shows that the amplitudes of head in the numerical model are less than or equal to exact values. Table 2 also shows that when $\Delta x \sqrt{(fs_c/K)}$ is larger than about 1.4, the error in the cell containing the well is more than 5%. When $\Delta x \sqrt{(fs_c/K)} > 5$,the error is larger than 43%, and the cell size is comparatively larger than the radius of influence of the well. The dynamics of water level fluctuation in the well at this point are dominated by the storage of water in the cell. Error ε_w is the smallest numerical error possible as time step $\Delta t \to 0$. Linear superposition can be used to compute the effects of multiple wells with steady and unsteady dumping rates.

In order to verify these results, a test is carried out with a 50 X 50 cell MODFLOW model with 2000 m square cells in a confined aquifer of $K/s_c = 500$, using a sinusoidal pumping rate of a variable pumping frequency f at the middle. About 200 pumping cycles were used first to obtain an initial condition for the test. About 200 more cycles were used to obtain the maximum amplitude in head for for a given frequency. The time step was selected so that $\psi < 0.08$, and therefore the time step is too small to cause significant errors. Table 3 shows the ε_w values obtained using the MODFLOW model, and the corresponding analytical values obtained using (31). It shows that the values agree well, and that the method can be used successfully to compute numerical errors in amplitude near groundwater wells. The results, which do not depend on actual dimensions, also indirectly confirm that the values of $a_c = 0.208$ and $a_a = 0.564$ used are sufficiently accurate. Errors in the numerical model can be larger because of errors of $O(\Delta t)$ and boundary effects. Errors further away from the well can be as large as the fraction of the amplitude. These errors can be determined approximately using (11).

NUMERICAL ERRORS UNDER STEADY STATE

Numerical errors under steady state due to disturbances caused by the source term can be determined by using methods similar to those used under unsteady conditions. Since steady state solutions are boundary dependent, a source term $S(x,y) = 2E_0Kk^2\exp(Ikx)\ \exp(Iky)$ is used to create a solution of (1) far away from the boundaries that can be solved both analytically and numerically. Such a source term can be introduced using a variable rainfall distribution. The analytical solution of the problem can be shown to be of the form $H(x,y) = E_0\exp(Ikx)\exp(Iky)$. To obtain the numerical solution, consider an arbitrary Fourier component $H_{i,j} = E\exp(I\phi i)\ \exp(I\phi j)$. Substituting

this component in the finite difference form of the governing equations, and computing the ratio of amplitudes of numerical and analytical forms, an estimate for the percentage error in amplitude can be estimated as

$$\varepsilon_s = 100\left(1 - \frac{\phi^2}{4\sin^2(\frac{\phi}{2})}\right) \approx -100\left(\frac{\phi^2}{12} + \frac{\phi^4}{240} + \dots\right) \tag{32}$$

in which, ε_s = steady state error as a percentage of the solution amplitude. The equation shows for example that ε_s exceeds 5% when ϕ exceeds 0.763. The corresponding values for 1% and 10% are 0.345 and 1.064 respectively. Equation (32) can be verified by making steady state runs for conditions with steady source terms having sinusoidal intensity variations. Model runs showed that the error equation can be verified up to 4 decimal places of precision.

NUMERICAL ERRORS NEAR WELLS UNDER STEADY STATE

Numerical errors are large near wells because of the curvature in the solution. The Thiem equation is used to compute the head distribution analytically when the water level in the cell containing the well is known. Thiem equation is expressed as

$$Q = 2\pi K \frac{H_2 - H_1}{\ln(r_2/r_1)} \tag{33}$$

in which, Q = pumping rate; subscripts 1 and 2 represent the well and the cell value respectively. $r_2 = 0.208\ \Delta x$ is used with square grids.

In order to represent numerical errors in dimensionless form, all the errors are normalized against the drawdown of the cell containing the well or the ”center cell”. The well is assumed to be positioned at the center of the square cell. The problem of determining the discretization then

becomes a problem in geometry, in which the error in drawdown is expressed in terms of $r_I/\Delta x$, in which r_I is the radial distance to a reference elevation or the radius of influence. The radius of influence can be computed using a number of empirical and semi-empirical equations outlined in the text by Bear (1972). For different values of $r_I/\Delta x$, the numerical error in the drawdowns of different cells including the cell containing the well can be obtained using numerical model runs. The drawdowns of different cells are measured with respect to a point at a radial distance r_I, and the errors are computed assuming that the drawdowns computed using (33) are exact. All errors are presented as percentages of the drawdown of the center cell, which is assumed to be equivalent to a well of diameter $0.208\Delta x$. A 50×50 cell grid was used to run the numerical model. Figure 6 shows the variation of the error obtained for cells at various distances. Three levels of discretization given by $r_I/\Delta x = 6$ and 14 along the axis and 7 along a diagonal are shown in the plots. All the plots in log scale follow an approximately linear behavior. If $r_I/\Delta x$ is less than about 7, the discretization is very coarse, and only a few points are available to make a plot in Figure 6 making such a plot less reliable. The percentage error in the figure can be expressed approximately using

$$\varepsilon = 2.07\exp\left(-0.726\frac{r}{\Delta x}\right), \quad \Delta x \le r < r_I \tag{34}$$

in which, $\varepsilon =$ error as a percentage of the drawdown in the center cell. The same equation can be written to express the absolute error as

$$H_\varepsilon = 2.07\left(\frac{Q}{2\pi T}\right)\log\left(\frac{r_I}{\Delta x}\right)\exp\left(-0.726\frac{r}{\Delta x}\right) \quad \Delta x \le r < r_I \tag{35}$$

These equations can also be used to obtain Δx for a model if the maximum error allowed at a distance r from the well is known. Superposition is possible with errors as with heads in the case of

multiple wells.

NUMERICAL ERRORS IN THE SOURCE TERM

Rainfall and evapotranspiration are considered as source terms in the equation governing overland and groundwater flow. The source term is a major contributor to stress, mainly in regional models when far away boundaries have only a limited dynamic influence. Stresses introduced through the source term create water level variations that are subject to errors during computations associated with the source term as well as other terms. A spatially and temporally varying rainfall pattern is used to study errors in the source term.

It can be shown that a solution in the complex form $H = H_0 \sin(Ikx + Iky - I f_I t)$ satisfies the governing equation (1) if the source term describing rainfall excess (rainfall - evapotranspiration) is expressed as $S = s_c H_0 \sqrt{(f_I^2 + f_k^2)} \cos(kx + ky - f_I t - \gamma))$ in which $k =$ the wave number; $f_I =$ frequency describing the rainfall pattern; $f_k = dKk^2$, $\gamma = \tan^{-1}(f_I / f_k)$. The above equation for H is used to obtain the analytical solution when computing numerical errors during the following experiments.

An analytical expression for the numerical error created by the source term is obtained by isolating the source term, determining the error generated by it, and combining with the error generated by the diffusion term. A solution of the form $H_0 \sin(f_I t)$ satisfies the truncated form of (1) without the second derivative terms when $S = s_c f_I H_0 \cos(f_I t)$. Consider the following weighted

implicit finite difference equation for the truncated equation.

$$H_i^{n+1} = H_i^n + \frac{\Delta t}{s_c}(\alpha S_i^{n+1} + (1-\alpha)S_i^n) \tag{36}$$

Numerical error in (36) can be computed by comparing the analytical solution corresponding to H_i^{n+1}, or $H_i(t+\Delta t)$, which is $H_0 \sin(f_I t + f_I \Delta t)$, with the numerical solution obtained by substituting $S_i^n = s_c f_I H_i \cos(f_I t)$ in (36). After algebraic manipulations, ε_I, the maximum numerical error introduced through the source term as a fraction of the amplitude can be expressed as a percentage of the amplitude as

$$\varepsilon_I = \sqrt{\psi_I^2 - 2\psi_I \sin\psi_I + 4\sin^2(\frac{\psi_I}{2})[1-\alpha(1-\alpha)\psi_I^2]} \tag{37}$$

in which, $\psi_I = f_I \Delta t$. For fully explicit and implicit methods, the expression reduces to

$$\varepsilon_I = \sqrt{\psi_I^2 - 2\psi_I \sin\psi_I + 4\sin^2(\frac{\psi_I}{2})} \approx \frac{\psi_I^2}{2} - \frac{\psi_I^4}{72} + \ldots \tag{38}$$

The ψ_I values corresponding to 1%, 5% and 10% errors are 0.448, 0.673 and 0.802 respectively. With central differencing, these numbers become 1.073, 1.413 and 1.593 respectively. The numerical error as a result of both the source term and the diffusion term is assumed to be

$$\varepsilon_r = \sqrt{\varepsilon^2 + \varepsilon_I^2} \tag{39}$$

in which ε is the error in one time step due to the diffusion terms alone, computed earlier using (8).

The accuracy of ε_r in (39) is tested by simulating the stress induced by two one dimensional rainfall patterns $N = N_0 \sin(kx - f_I t))$ traveling in opposite directions. The value of β required to estimate ε is computed using $\beta = \psi_k/\phi^2$ in which, $\psi_k = f_k \Delta t$ and $f_k = Kk^2/s_c$. Figure 7 shows

the variation of the numerical error for a fully implicit 1-D model under such source induced flow conditions. Results are shown for two sets of ϕ and β values. Up to 20 cycles of spatial waves were simulated in the experiment using 100 grid points. Over 4000 time cycles were used to create the initial condition before the experiment was carried out as before. The figure shows that the numerical and analytical estimates agree approximately.

APPLICATION TO AN EXISTING MODEL IN SOUTH FLORIDA

A number of hydrologic models are used in South Florida to solve problems of various space and time scales. These models are based on the same governing equations, and have many similar characteristics. The South Florida Water Management Model (SFWMM) (SFWMD, 1997, Fennema, et al., 1994) developed by the South Florida Water Management District (SFWMD) is one of the regional models used in the area. SFWMM is a physically based overland and groundwater flow model. It simulates flow over a very large part of South Florida. The model uses a 3.2 km (2 mile) square grid, and a 6 hr. time step. Time series data for the boundary conditions and the source term are provided at 1 day time steps. In order to evaluate the validity of the diffusion flow assumption in the model, first consider somewhat extreme values of water depth $h = 1$ m, and slope $S_0 = 2\text{–}5\times10^{-5}$ in the Central and Southern Everglades during wet periods. These values can be used to compute the wave period of the shortest Fourier component that can be simulated, using $T_p = 30\sqrt{(h/g)}/S_0 \approx 4$ days, as suggested by Ponce (1978). This equation is based on a maximum amplitude error of 5%. The equation shows that the diffusion assumption is valid unless events of shorter duration are simulated. If however the slopes are large, and the depths are low as in certain areas of the Everglades, the model can simulate events of shorter duration using finer

discretizations.

The 3.2 km (2 mi) grid and the 6 hr time step in the SFWMM can represent various Fourier components in the solution with various accuracies. Table 4 shows errors of representation described in type (A) or (B) for different Fourier components, computed using (5) and (6). It shows that the SFWMM can represent Fourier components of wavelength as small as 18 km and period as small as 5.7 days with an accuracy of 5%. Using a typical high value of $K = 250\ m^2/s$ for overland flow obtained using $h \approx 1\ m$, $S_0 \approx 2 \times 10^{-5}$ and $n_b \approx 1$ for the deep portions of the Everglades, a Fourier component of wave length 18 km in space can be shown to be associated with a wave period of 2.5 days in time according to $f = 2Kk^2$. The time step required to represent a Fourier component of period 2.5 days with a maximum error of 5% is approximately 0.4 days. In the case of groundwater, assuming a typical high value of $K = 8\ m^2/s$ found near the Lower East Coast of South Florida, Fourier components of period 77 days and larger can be represented using the same spatial grid. Data presented at 14 day intervals are sufficient to describe stresses of this period. Any high frequency component in the groundwater flow generated by daily data is not supported by the spatial grid.

In order to compute the numerical error due to water level changes at internal and external boundaries, consider a water level fluctuation of amplitude 1 m and period 6 days near a canal as an example. The amplitude at a distance of 6.4 km or two cells is computed by first obtaining k using $f = 2Kk^2$ as $1.557 \times 10^{-4} s^{-1}$ and then using (16). The amplitude at the distance is

$1.0 \times e^{-kx} = 0.37$ m. Assuming that $\phi = k\Delta x = 0.5$, β can be shown to be 0.52. Since $\beta > 0.25$, it can be seen that an explicit model is unstable under the conditions. For an implicit model, the error is approximately $(1/2)kx\phi^2\beta$ or 6.5% of the amplitude, and the absolute error is 6.5% of 0.37 m or 24 mm. The percentage error in discharge for this case is also approximately 6.5%. The error is largest when $fT = 1$, or at a distance of 7 km.

The error due to rain driven water level fluctuations is proportional to the rainfall intensity. In South Florida, this is one of the largest driving forces of hydrology, and also the largest potential source of error in models. For a stationary rainfall intensity pattern described by a period of 12 days and a wave length of 18 km for example, $\psi_I = f_I\Delta t = 0.524$, and the error $\varepsilon_I = 13.6\%$ according to (37). For the stresses induced by this rainfall, $\phi = 1.1$, and $\beta = 0.52$ which gives $\varepsilon_T = 6.7\%$ when using $fT = \pi/4$ and (12). The total numerical error due to both source term and diffusion term computations as a result of rain driven flow can now be computed using (39) to give 15.2%. If the wave length of the rainfall density pattern is 18 km or less, the rainfall data has to be collected with a spatial resolution of 3.2 km to maintain a <5% error in the input data interpretation. When rainfall data is collected at a lower resolution, the model will contain only the corresponding lower frequency components. In South Florida, short duration small scale rainfall events account for a large part of the total rain, and have to be represented accurately if these components are to be represented accurately in models.

To demonstrate the accuracy of the SFWMM in simulating water levels near a pumping well,

use Table 2 and select $\Delta x\sqrt{(fs_c/K)} < 1.4$ for the error in the center cell to be less than 5%. With 3.2 km cells and $K = 8\ m^2/s$ for groundwater, this corresponds to a pumping cycle of period > 48 days. This example shows that heads computed near a well have large errors except in cases where the pumping rates change very slowly. Table 1 shows that the amplitude decays to less than 0.5% after 5 cells. The steady state error is less that 1.1% of the steady state drawdown of the center cell.

The numerical error in the final model output is a combination of errors in various steady and unsteady state stress components. When the numerical error is needed at a given point in the model, the first step is to find the sources of the stresses, and their spatial and temporal characteristics. When they are found, the principle of superposition can be used to find the errors due to each of the stresses. In many parts of the Everglades, stresses are mainly due to rain and canal level fluctuations that result from the operation of pumps and water control structures.

SUMMARY AND CONCLUSIONS

The study shows that numerical errors resulting from spatial and temporal discretizations can be explained using dimensionless variables ϕ and β respectively. The results shows that the error generally increases with both ϕ and β. For a given spatial discretization ϕ, it can be shown that the error cannot be reduced below a certain value unless ϕ is also reduced. Similarly, the error for a given β cannot be reduced unless ϕ too is reduced. Using $\phi < 1.1$ and $\psi < 1.1$ in the case of 1-D, errors of spatial and temporal discretization can generally be kept below 5%. Using numerical experiments with explicit models and implicit models such as MODFLOW, and using variable boundary water levels, variable rainfall patterns and variable well pumping rates, it was possible

to show that numerical errors in a variety of finite difference models can be computed using the proposed analytical equations. Test results also show that the analytical error estimates obtained for steady state problems with a steady rainfall pattern are accurate. Numerical errors other than amplitude errors resulting from material heterogeneities, discontinuities, or boundary effects are not considered in the study.

In the case of the experiment using a variable boundary water level, the results show that the maximum error as a percentage of the amplitude increases linearly with distance from the boundary. The results also show that the maximum error in the discharge behaves similarly. By using a steady water head profile generated by a steady rainfall pattern, it was possible to show that $\varepsilon_s >$ 5% if $\phi > 0.763$. By using rainfall patterns changing with time, it was also possible to show that the error ε_I in computations involving the source term is >5% when $\psi_I > 0.673$ where ψ_I describes the temporal discretization of the rainfall. Using pumping experiments carried out at a cell in the MODFLOW model, it was shown that the numerical value of the amplitude in the cell containing the well decreases with increasing cell size, and the error > 5% when $\Delta x > 1.4\sqrt{(K/fs_c)}$. Results using a steady state pumping problem show that the error in the drawdown of the cell containing the well when $r_w = 0.208\Delta x$ is about 1%, and reduces rapidly with radial distance. A summary of some of the practically useful equations obtained during the study are shown in Appendix A. The study shows that sufficient spatial discretizations and matching temporal discretizations must be used if a given Fourier component is to be represented accurately in a model.

ACKNOWLEDGMENTS

The writer thanks Mark Belnap for the MODFLOW runs, and Joel VanArmen for reading and reorganizing the manuscript. Review comments by Jayantha Obeysekera, Todd Tisdale, Victor Kelson, Randy Van Zee, Ken Tarboton and Matt Hinton of the Hydrologic Systems Modeling group of the South Florida Water Management District were extremely useful. The writer specially thanks Dr. Richard Cooley, and other reviewers of Water Resources Research for the review and the excellent suggestions.

APPENDIX A

A Summary of practically useful equations

Table A.1: Practically useful formulas in approximate form. In the equations, f = frequency of the disturbance in water level; K = transmissivity of the aquifer.

Equation	Reference
$X\sqrt{(fs_c/K)} = 4.3$	X is the distance at which a 1-D disturbance of frequency f would decay to 5% of the amplitude.
$\Delta x = 1.1\sqrt{K/fs_c}$	Δx gives the spatial discretization needed to represent a water surface profile with 5% accuracy. The profile is created by a disturbance of frequency f.
$\Delta x = 0.5\sqrt{K\varepsilon_d/fs_c}$	Δx needed to represent the same spatial discretization with a ε_d % accuracy.
$K\Delta t/\Delta x^2 s_c = 0.14$	Δt gives the time step needed if the numerical error is limited to 5% of the disturbing amplitude.

$\Delta x\sqrt{(fs_c/K)} < 1.4$	Δx gives the size of a square cell needed to solve the amplitude of a well fluctuation with a maximum error of 5%.
$\Delta x\sqrt{(fs_c/K)} = 5$	gives a practically useful upper bound of Δx that can be used to model a pumping well (error $< 40\%$).
$r\sqrt{(fs_c/K)} = 2.75$	r is the radius at which the amplitude of a well with $\hat{r}_w = 0.5$ decays to 5% of the amplitude of the well.
$\varepsilon = 2.07\exp(-0.726r/\Delta x)$	ε gives the numerical error of a steady state well as a percentage of the drawdown.

APPENDIX B

Definition of variables

Variable	Definition
A	area simulated by the model (m^2).
f_I	frequency of the rainfall pattern.
g	gravitational acceleration.
h	water depth, (m).
H	water level or water head (m).
H_ε	error in the steady state solution near a well.
K	transmissivity of aquifer for groundwater flow; $h^{\frac{5}{3}}/(n_b\sqrt{S_n})$ for overland flow, m^2/s.
K_0, K_1	modified Bessel functions of type 0 and 1.
r	radial distance from the center of a well.
$\hat{r}$	$= r\sqrt{(fs_c/K)} =$ dimensionless r.
$\hat{r}_w$	well radius in dimensionaless form.
S	source term representing rainfall and evapotranspiration.
s_c	storage coefficient
T	time during which a harmonic in the solution evolves, (s).
x, y	distances along x, y coordinate axes, (m).
X	distances at which a disturbance is measured, (m)
α	time weighting factor in the weighted implicit scheme.

Variable	Definition
β	$K\Delta t/(s_c\Delta x^2)$, dimensionless time step.
ΔA	area of a cell, (m^2).
Δx	size of a square cell.
ε	maximum local numerical error per one time step as a fraction of the local amplitude.
ε_Q	numerical error in discharge as a percentage of discharge.
ε_s	numerical error due to computations associated with the source term, as a fraction of the local amplitude.
ε_T	maximum local numerical error as a fraction of the local amplitude.
ϕ	dimensionless spatial discretization defined as $k\Delta x$.
ψ	a dimensionless time discretization defined as $f\Delta t$.
ψ_I	a dimensionless time discretization defined as $f_I\Delta t$.

REFERENCES

Anderson, M. P. and Woessner, W. W. (1991). "Applied groundwater modeling, simulation of flow and convective transport", *Academic Press, Inc.*, New York.

Bear, J. (1979) "Hydraulics of Groundwater", *McGraw Hill*, New York.

Burden, R. L. and Fairs, J. D. (1985). *Numerical analysis*, Third Edition, Prindle, Weber & Schmidt, Boston, MA.

Dongarra, J. J. (1998). "Performance of various computers using standard linear equation software", *Computer Science Dept. University of Tennessee*, Report CS-89-85, Knoxville, TN.

Feng, Ke, and Molz, F. J. (1997). "A 2-D diffusion based wetland model", *Journal of Hydrology*, 196(1997), 230-250.

Fennema, R. J., Neidrauer, C. J., Johnson, R. A., MacVicor, T. K., Perkins, W. A. (1994). "A computer model to simulate natural Everglades hydrology", *Everglades, The Ecosystem and its restoration*, Eds. Davis, S. M. and Ogden, J. C., St. Lucie Press, FL, 249-289.

Fitz, H. C., DeBellevue, E. B., Costanza R., Boumans, R., Maxwell, T., Wainger, L. and Sklar, F. H. 91996). "Development of a general ecosystem model for a range of scales and ecosystems", *Ecological Modeling*, vol 88, 263-295.

Haitjema, H. M. (1995). "Analytic element modeling of groundwater flow", *Academic Press*, New York.

Hirsch, C. (1989). *Numerical computation of external and internal flows*, John Wiley & Sons, Inc., New York, N.Y.

Hromadka II, T. V., and Lai, Chintu, (1985). "Solving the two-dimensional diffusion flow

model", *Proc. of the Specialty Conf. sponsored by the Hydraulics Div. of ASCE*, Lake Buena Vista, FL, Aug 12-17.

Lal, A. M. W. (1995). "Calibration of riverbed roughness", *J. Hydr. Div.*, ASCE, 121(9), 664-670.

Lal, A. M. W. (1998a). "Performance comparison of overland flow algorithms", *J. Hydr. Div.,* ASCE, 124(4), 342-349.

Lal, A. M. W. (1998b). "A weighted implicit finite volume model for overland flow", *J. Hydr. Div.,* ASCE, 124(9).

McDonald, M. and Harbough, A. (1988). "A modular three dimensional finite difference groundwater flow model", Report 06-A1, *US Geological Survey, Reston, VA*.

Neuman, S. P. (1973). "Calibration of distributed parameter groundwater flow models viewed as a multiple objective decision process under uncertainty", *Water Resources Research*, 9(4), 1006-1021.

Richtmyer, R. D. and Morton, K. W. (1967). *Difference methods for initial value problems*, Second Edition, J. Wiley and Sons, New York, NY.

SFWMD, (1997). "Documentation of the South Florida Water Management Model", Draft Document, South Florida Water Management District, West Palm Beach, FL.

Sod, G. A. (1985). Numerical methods in fluid dynamics, *Cambridge University Press*, Cambridge, UK.

Strack, O. D. L. (1989). Groundwater mechanics, *Prentice Hall*, NJ. Townley, L. R. (1995). "The response of aquifers to periodic forcing", *Advances in Water Resources*, vol 18, 125-146.

Willis R. and Yeh, W. W. G. (1987). Groundwater systems planning and management, *Prentice-Hall*, NJ.

FIGURE CAPTIONS

Figure 1: Variation of numerical error and amplitude with distance from the boundary for the MODFLOW model.

Figure 2: Variation of numerical error with spatial and temporal resolutions for the ADI method. Lines show analytical values and symbols show values observed in the model.

Figure 3: Variation of numerical error with spatial and temporal resolution for the explicit method. Lines show analytical values and symbols show values observed in the model.

Figure 4: Variation of numerical error with spatial and temporal resolutions for the MODFLOW model. Lines show analytical values and symbols show values observed in the model.

Figure 5: Variation of error in discharge for a fully implicit model. Lines show analytical values and symbols show values observed in the model.

Figure 6: Variation of steady state numerical error with radial distance.

Figure 7: Variation of error in the source term with ψ_I. Lines show analytical values and symbols show values observed in the model.

Table 1: Amplitudes of water level fluctuations given by (26) for various well radii $\hat{r}_w = a_c \Delta x \sqrt{(f s_c / K)}$ representing various discretizations. Values of $K_0(\hat{r})/(\hat{r}_w K_1(\hat{r}_w))$ are shown in the table. $a_c = 0.208$.

	$\hat{r}$							
$\hat{r}_w$	0.01	0.05	0.1	0.5	1.0	2.0	5.0	10.0
0.01	4.722	3.115	2.428	0.925	0.421	0.114	0.004	1.8×10^{-5}
0.05		3.128	2.438	0.929	0.422	0.114	0.004	1.8×10^{-5}
0.1			2.463	0.938	0.427	0.115	0.004	1.8×10^{-5}
0.5				1.116	0.508	0.137	0.004	2.0×10^{-5}
2.0						0.407	0.013	6.0×10^{-5}

Table 2: Variation of ε_w, the error in the amplitude of the cell containing a well as a percentage of its exact amplitude, with dimensionless Δx for a square grid. C_c, the ratio between amplitudes is also shown.

$\Delta x\sqrt{(fs_c/K)}$	0.01	0.02	0.05	0.1	0.2	0.5
C_c	1.0000	0.9999	0.9997	0.9990	0.9967	0.9844
ε_w (%)	$4.200\ 10^{-7}$	$5.130\ 10^{-5}$	$1.351\ 10^{-4}$	$1.508\ 10^{-3}$	$1.564\ \ 10^{-2}$	0.289

$\Delta x\sqrt{(fs_c/K)}$	1	2	5	10	20
C_c	0.9523	0.8886	0.5640	0.2563	$4.3228\ \ 10^{-2}$
ε_w (%)	2.13	11.1	43.6	74.4	95.7

Table 3: Comparison of values of ε_w obtained analytically and using the MODFLOW model.

$\Delta x\sqrt{(fs_c/K)}$	0.54	1.53	6.10	8.63
ε_w (analytical)	0.4%	6%	52%	68%
ε_w (MODFLOW)	4%	5%	71%	82%
ϕ	0.27	0.76	3.05	4.31

Table 4: Characteristics of various 1-D and 2-D Fourier components that can be represented by using a 3.2 km (2 mile) grid cell and a 1 day time step.

Wave length (1-D) (km)	41	18	13	6	4	19
Wave length (2-D) (km)	57	25	18	8	5	27
Max. error (%)	1%	5%	10%	50%	100%	4.5%

Wave period (Days)	12.8	5.7	4.1	1.8	1.3	6
Max. error (%)	1%	5%	10%	50%	100%	4.5%

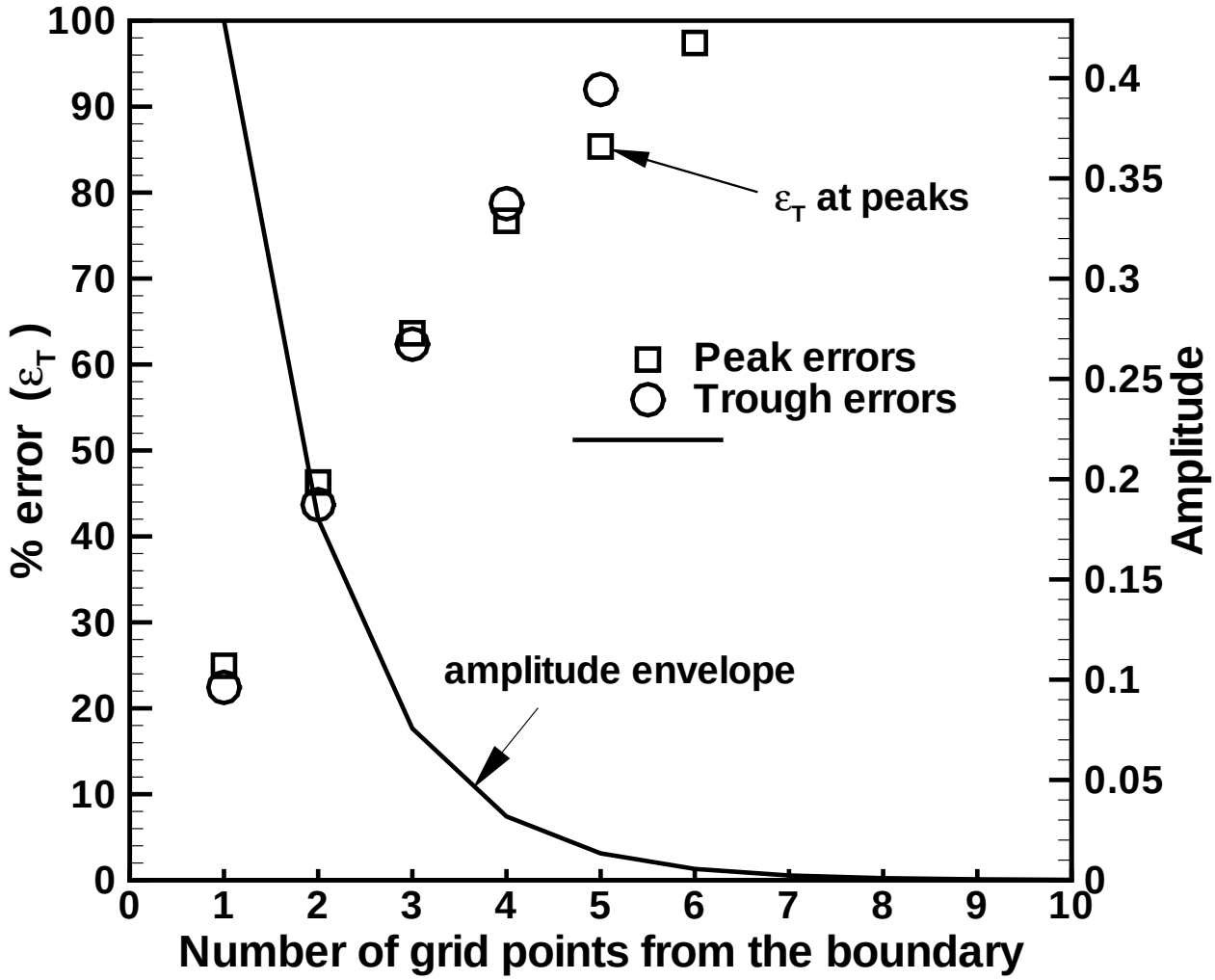

Figure 1: Variation of numerical error and amplitude with distance from the boundary for the MODFLOW model.

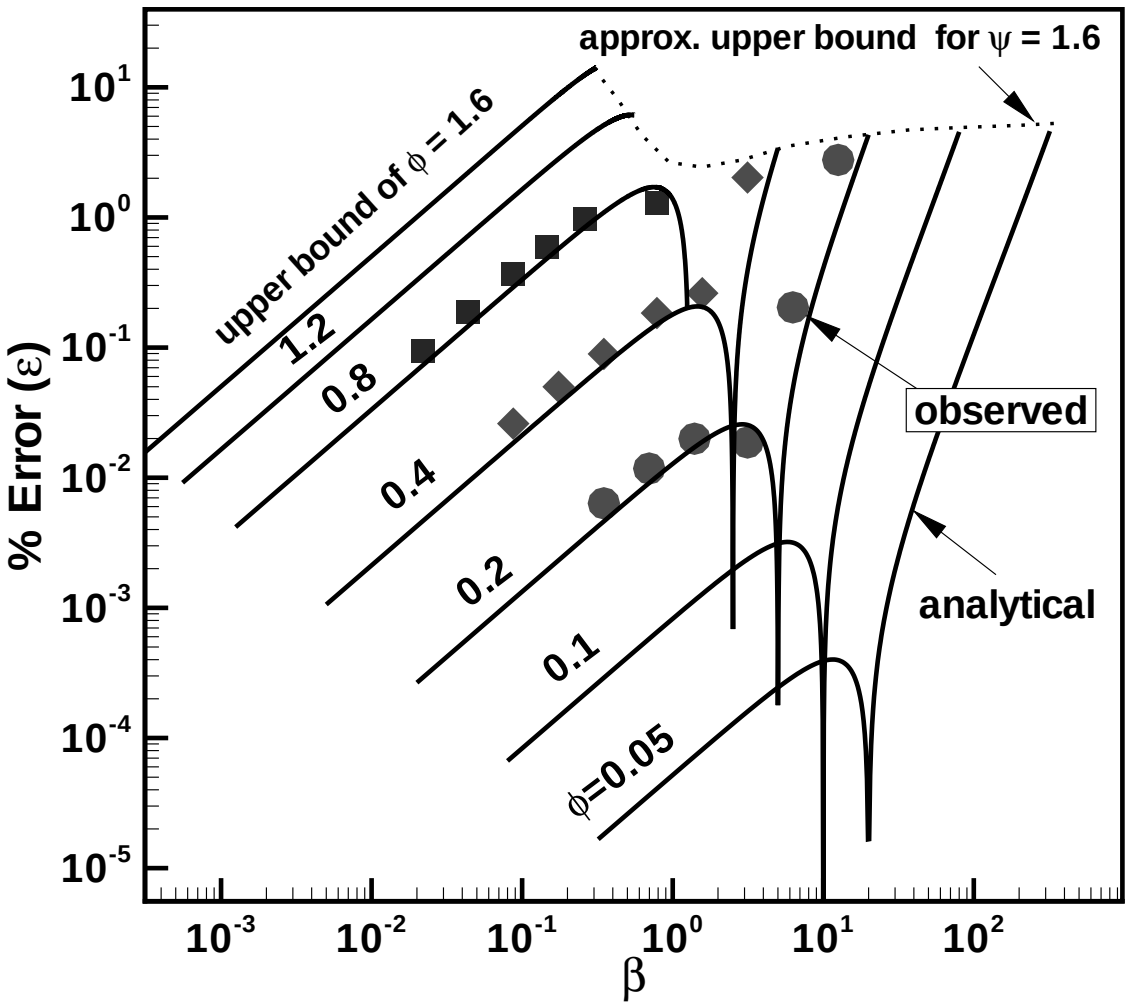

Figure 2: Variation of numerical error with spatial and temporal resolutions for the ADI method. Lines show analytical values and symbols show values observed in the model.

/usr2/wlal/resolution/exper_xp.lay

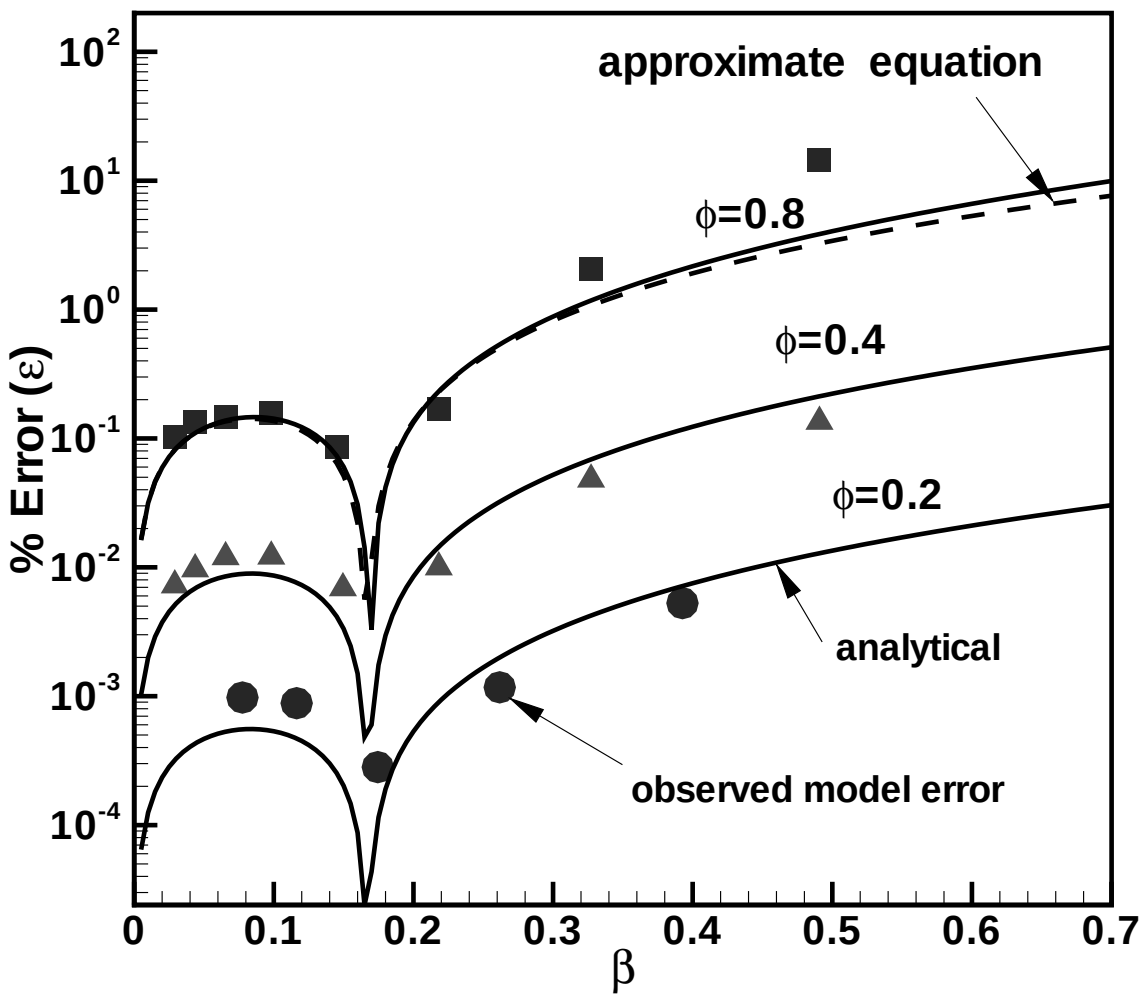

Figure 3: Variation of numerical error with spatial and temporal resolution for the explicit method. Lines show analytical values and symbols show values observed in the model.

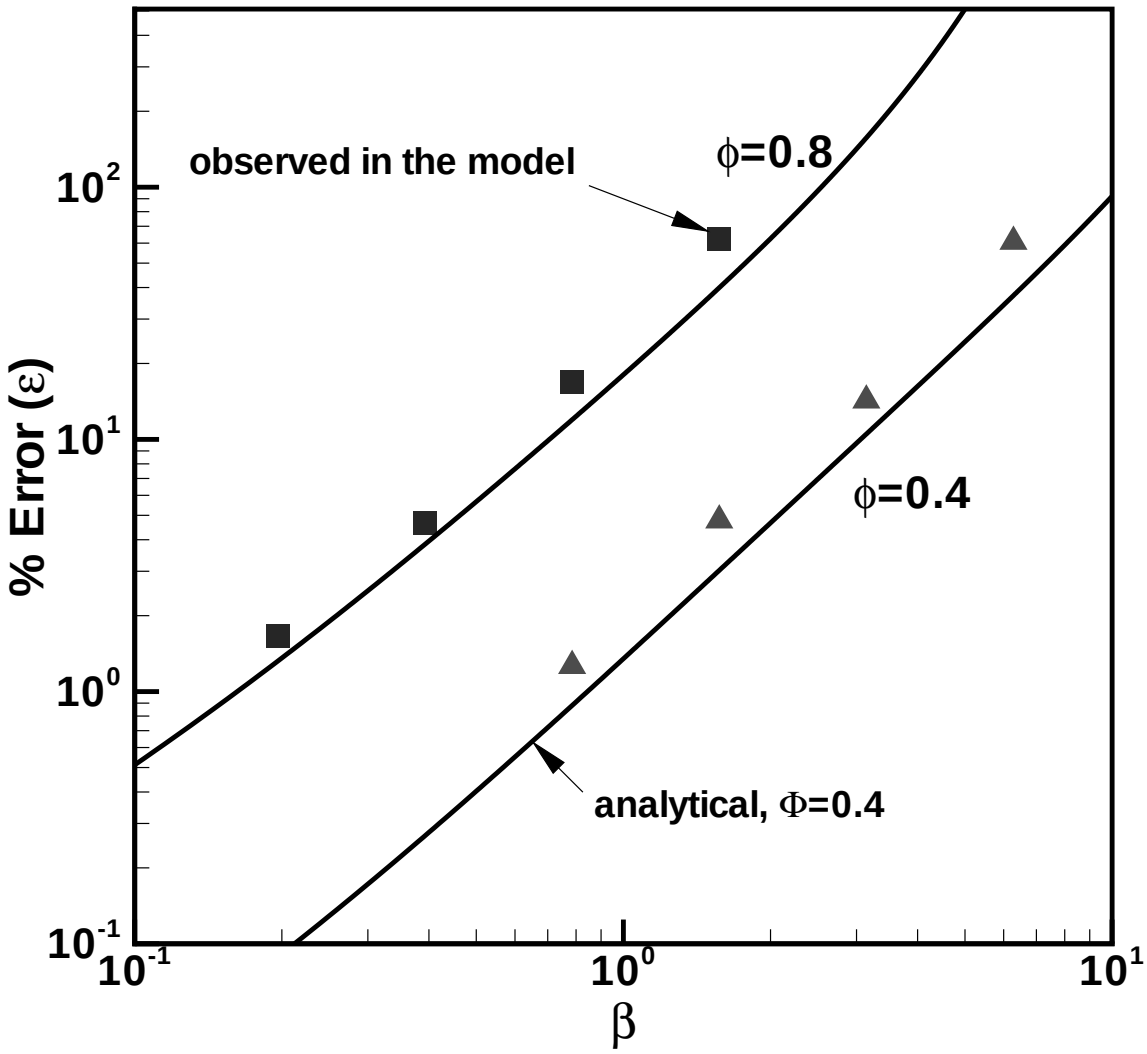

Figure 4: Variation of numerical error with spatial and temporal resolutions for the MODFLOW model. Lines show analytical values and symbols show values observed in the model.

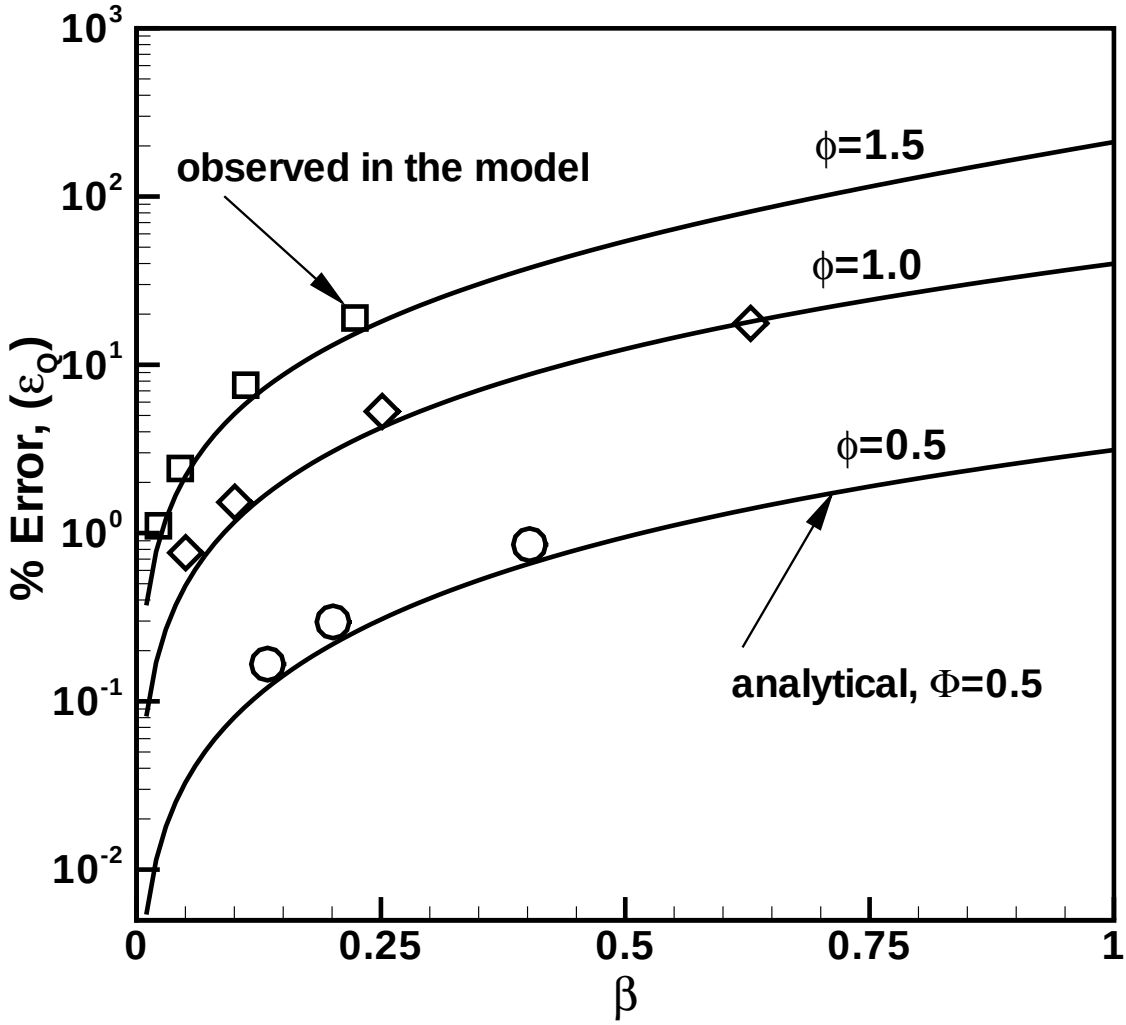

Figure 5: Variation of error in discharge for a fully implicit model. Lines show analytical values and symbols show values observed in the model.

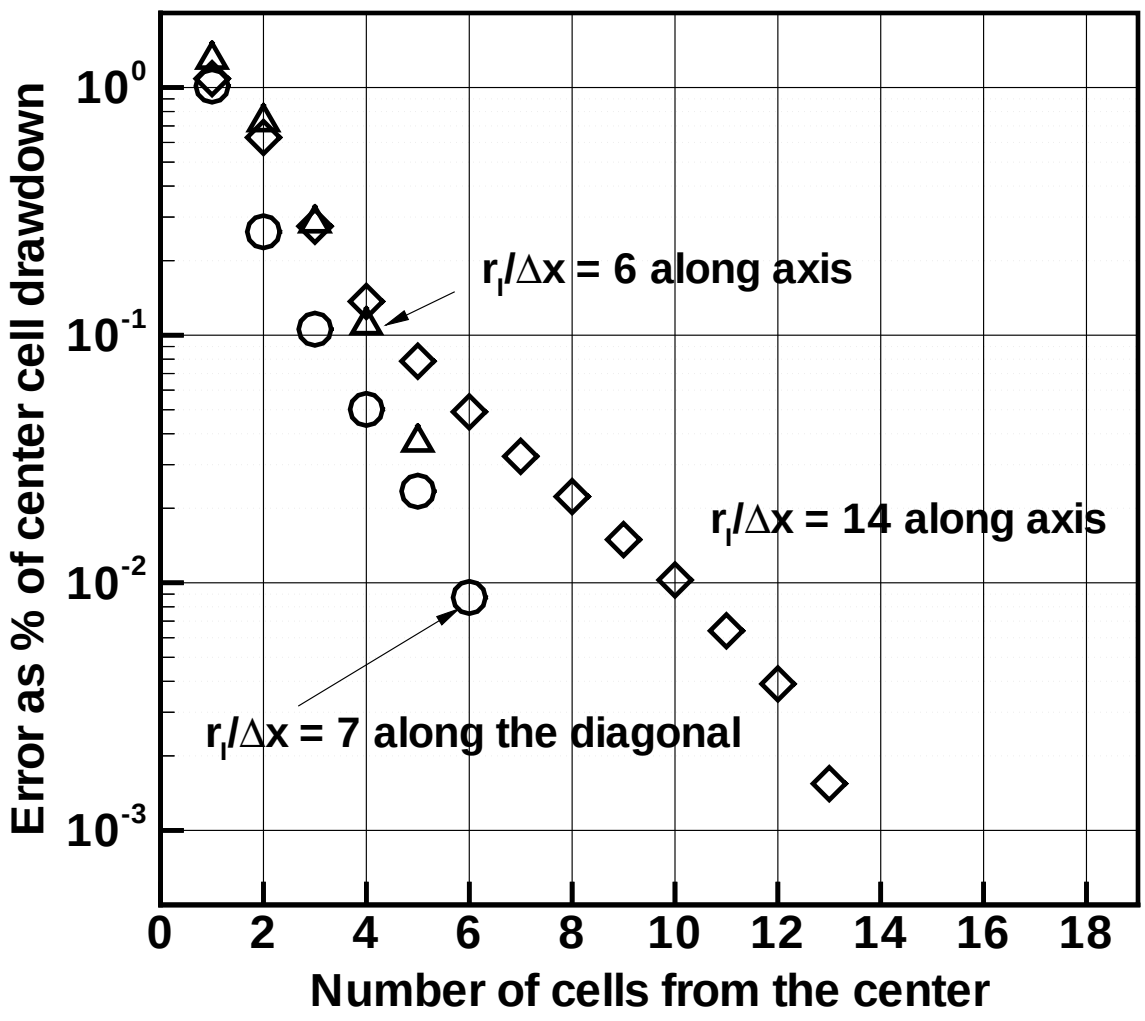

Figure 6: Variation of steady state numerical error with radial distance.

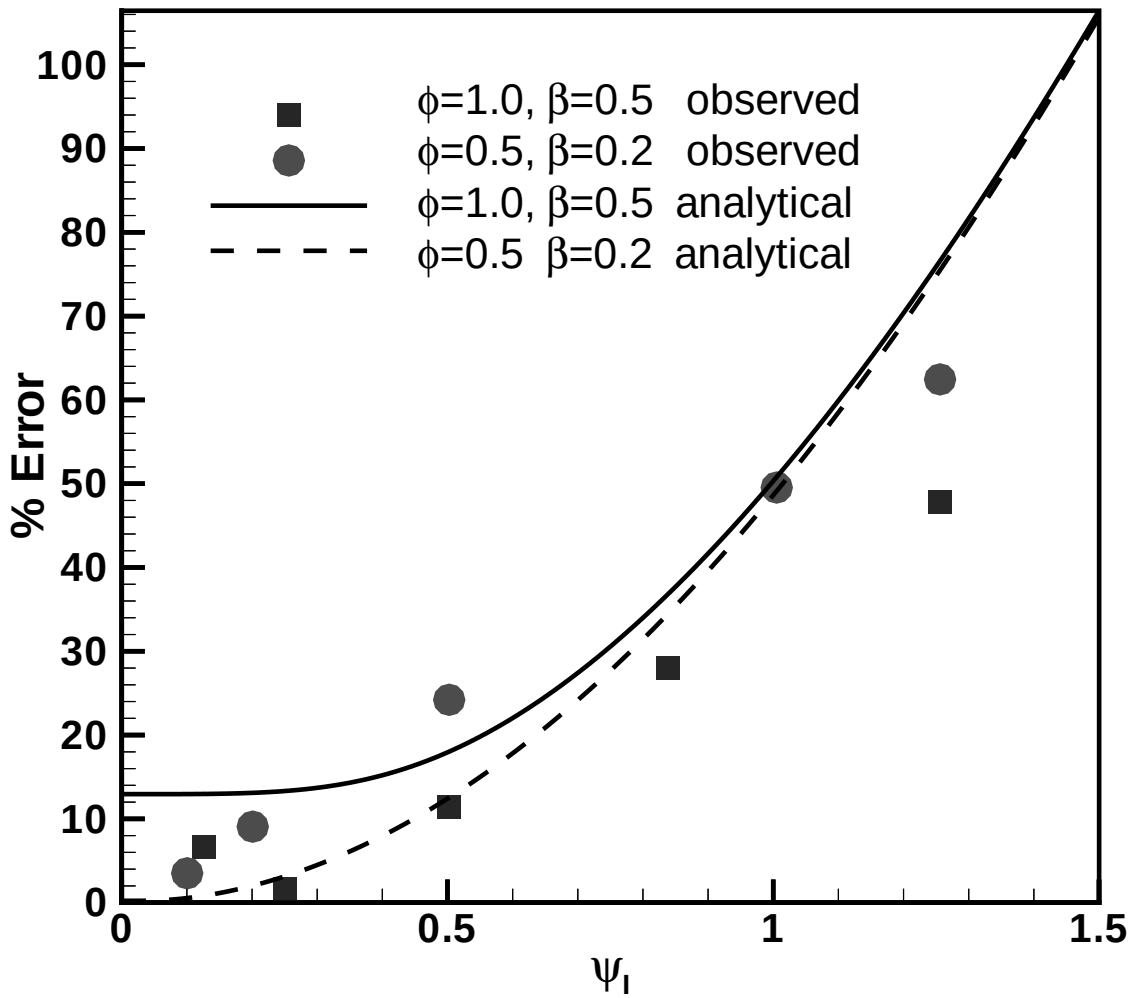

Figure 7: Variation of error in the source term with ψ_I. Lines show analytical values and symbols show values observed in the model.